Nanoelectromechanical devices with carbon nanotubes

Cite as:
Lee, S., & Campbell, E. (2013). Nanoelectromechanical devices with carbon nanotubes. *Current Applied Physics*, 13(8), 1844-1859.

Manuscript received: 13/02/2013; Accepted: 28/02/2013; Article published: 23/04/2013

Nanoelectromechanical devices with carbon nanotubes**

Sang Wook Lee[1] and Eleanor E.E.B. Campbell[1,2]

[1]Division of Quantum Phases and Devices, School of Physics, Konkuk University, 143-701 Seoul, Republic of Korea.

[2]EaStCHEM, School of Chemistry, Joseph Black Building, University of Edinburgh, West Mains Road, Edinburgh, EH9 3JJ, UK.

[*]Corresponding authors; S.W.L. e-mail: leesw@konkuk.ac.kr; E.E.B.C. e-mail: Eleanor.Campbell@ed.ac.uk

[**]We would like to thank all our students and collaborators over the years who have contributed to our CNT/CNF NEMS research, in particular our theoretical collaborators, Jari Kinaret and Andreas Isacsson from Chalmers University of Technology. This work was supported through BSR (2011-0021207, 2012R1A2A2A01045496), NMTD (2012M3A7B4049888), WCU (R31-2008-000-10057-0), and the framework of international cooperation programs (2012K2A1A2032569) supported by the National Research Foundation of Korea (NRF) funded by the Ministry of Education, Science and Technology.

Abstract:
Thanks to their excellent mechanical properties as well as interesting electrical characteristics, carbon nanotubes are among the most widely used materials for the study of electromechanical properties. This review paper presents the physical properties and the potential applications of carbon nanotube based nanoelectromechanical devices. We present an overview of fabrication methods followed by a discussion of the physical properties of CNT-NEMS. Finally some potential applications are discussed.

Keywords:
Carbon nanotube; Nanoelectromechanical system; Nano fabrication

Contents

1. Introduction

1.1. Nanoelectromechanical system (NEMS)

Most students who learn general physics will know how Charles-Augustin de Coulomb performed his experiment in 1777 to measure the electrostatic force. Coulomb used an electrically charged torsional pendulum and an oppositely charged stick to generate the electrostatic force. That experimental set up could be the first well-defined electromechanical system. In 1798, Henry Cavendish carried out a similar experiment to determine the gravitational constant, however, his instrument should more accurately be classified as an ‘opto’-mechanical system. Sketches of the two experiments are shown in Fig. 1. With these techniques, the two physicists were able to accurately determine the Coulomb constant and the gravitational constant over 200 years ago from considering the relation between very small forces. From this we learn that by making use of the coupling between the electrical (or optical) and mechanical degrees of freedom, it is possible to carry out ultrasensitive measurements.

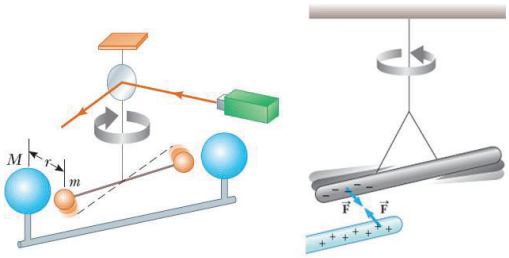

Figure 1. Schematics of Cavendish's (a) and Coulomb's (b) torsional valence [1] (From SERWAY/JEWETT. Principles of Physics, 4E. © 2006 Brooks/Cole, a part of Cengage Learning, Inc. Reproduced by permission. www.cengage.com/permissions)

Thanks to the recent developments of nano fabrication techniques, we are able to reduce the size of electromechanical systems down to the nanometer scale. This has allowed the flourishing of a new field of research devoted to the study of nanoelectromechanical systems (NEMS). [2] NEMS are composed of a nanoscale mechanical system in combination with electrical components. The mechanical system transduces the electrical stimuli to mechanical responses and also the mechanical motions to electrical signals. The electrical components give stimuli and receive response signals by electrical means. Figure 2 illustrates the concept of NEMS.

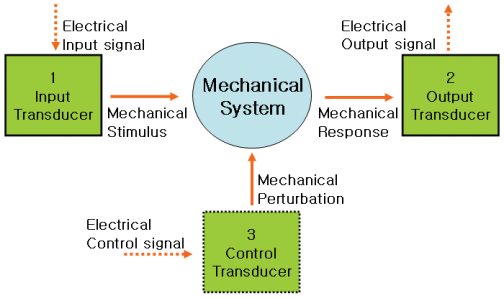

Figure 2.Concept of nano-electromechanical system (NEMS)[2] (Reprinted with permission from Rev. Sci. Inst. 76, 061101 (2005). Copyright 2005 American Institute of Physics.)

Notable physical differences will occur when the size of the electromechanical device is reduced down to the nanoscale. First of all, one can study quantum mechanical phenomena with nanoelectromechanical systems [3]. Ultrasensitive sensing is also possible from the mechanical and electrical coupling of nanoscale electromechanical systems [4, 5].

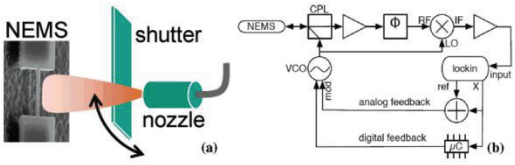

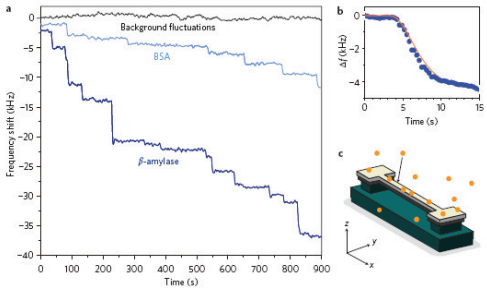

Figure 3.Sensitive gas detector (upper) [4] (Reprinted with permission from Nanolett. 6, 583 (2006). Copyright 2006 American Chemical Society.) and single molecular detector (bottom) using Si based NEMS [5](Reprinted with permission from Nat. Nano.4, 445 (2009). Copyright 2009 Nature Publishing Group.)

The different behavior of electromechanical systems on the nanoscale is largely due to their ability to mechanically respond with high frequency (or speed) and the improvement in the Q-factor as the size of the system is reduced. The mechanical performance of the system can also be enhanced by using mechanically strong but light-weight nanomaterials.

1.2. CNT based NEMS

A carbon nanotube (CNT) is a one-dimensional nanostructure which can be thought of as a graphene sheet rolled up into a cylinder [6]. The electrical properties of CNT are either metallic or semiconducting according to the chirality i.e. the wrapping angle of the carbon atoms around the nanotube axis. Numerous papers reporting the electrical properties and the possible applications of CNT have been published since their breakthrough in 1991. As well as the interesting electrical properties, CNTs also have excellent mechanical properties. CNTs are unique one-dimensional structures in which high flexibility and high strength coexist; they can sustain their structure under strain leading to a 20% elongation [7] and have a Young's modulus of around 1 TPa [8]. Thanks to these superior mechanical properties combined with a low density (around 6 times lower density than steel), CNTs are already used to enhance the mechanical strength of commercially available products we come across in ordinary everyday life such as tennis rackets, golf clubs, and so on. As discussed in the previous section, excellent performances of NEMS can be realized when we use strong materials. Since CNT have outstanding mechanical and electrical properties, they are considered to be among the most promising candidates as building-blocks for NEMS.

Figure 4 shows the structure of a CNT-based resonator. The resonance frequency of the suspended SWNT with high Q factor (up to 150,000) sensitively shifted on addition of an electron to the nanotube. The softening of the mechanical spring constant of the CNT occurred due to charge fluctuations at the single electron level on the CNT quantum dot. (See ref [9] for detailed explanations and further discussion in section 3.)

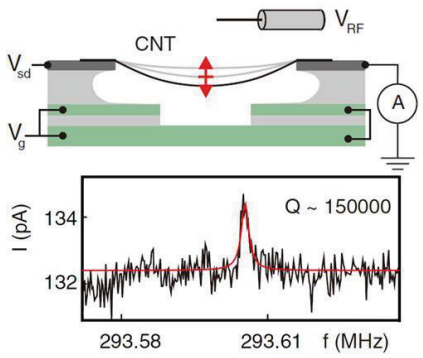

Figure 4. Doubly clamped CNT based resonator with high Q factor (up to 150,000) and its electromechanical coupling behavior.[9] (Reprinted with permission from Science 325, 1103 (2009). Copyright

2009 American Association for the Advancement of Science.)

1.3. Outline of paper

In this paper, we will review the fabrication and the physical properties of carbon nanotube based nanoelectromechanical devices. Several fabrication procedures for producing suspended carbon nanotube structures with mechanical degrees of freedom will be introduced in the following section of this paper. Then, the basic mechanical and electromechanical properties of the devices are presented. Finally, the possible applications of CNT based NEMS will be introduced, followed by a discussion of future prospects of CNT based NEMS.

2. Device fabrication

To fabricate a nanoelectromechanical system using CNT, we first have to make the CNT suspended in order to allow for mechanical motion of the CNT. Several approaches for producing suspended CNTs have been reported. The most widely used method to make the suspended structure is to etch the substrate after connecting the CNT to electrodes.[10, 11] With this process, since the substrate is etched by a strong acid such as HF, special care should be taken. Apart from the safety issue, there is also the limitation of selecting nanomaterials to make the suspended structures. This method cannot be more generally applied to other low dimensional nanostructures which can be destroyed by the etchant.

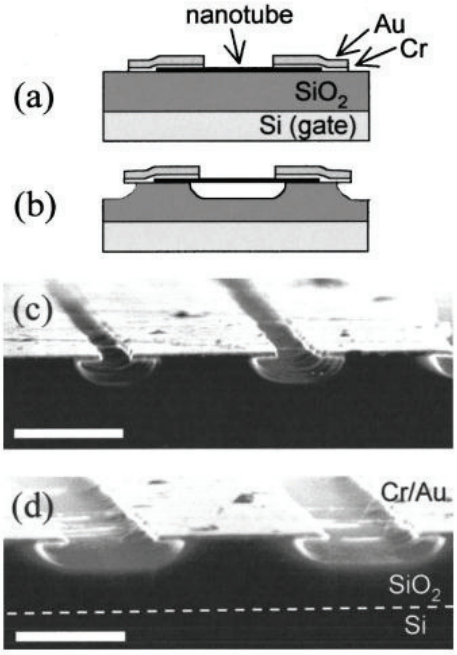

Figure 5.Suspended CNT structures produced by wet etching.[11] (Reprinted with permission from Appl. Phys. Lett. 79, 4216 (2001). Copyright 2001 American Institute of Physics.)

Figure 5 shows suspended SWNT structures which were fabricated by a wet etching process. In this case, carbon nanotubes are first dispersed or deposited on the substrate. The metal anchor structures are defined by electron beam evaporation on top of the SWNTs after an electron-beam or photo-lithography process. The material for the anchors should be resistive to the etchant in order to support the suspended SWNTs after the underlying substrate is etched. Then the chip is immersed in a buffered SiO_2 wet etch. Buffered HF is generally used to etch the SiO_2. After the wet etching process, the whole chip is rinsed by water and isopropanol, followed

by nitrogen blowing. Critical point drying is used to avoid the CNT being pulled down due to surface tension effects during the drying process.

This is one of the "traditional" methods to fabricate suspended nanostructures since the process itself is simple. Most of the CNTs can be well-suspended after the wet etching and drying process. However wet etchants etch the substrate isotropically, leading to a large undercut being created under the suspended SWNTs. In this case, the distance between the anchoring metal patterns does not necessarily define the exact suspended length of the CNTs since the CNTs are often not tightly attached to the metal area where the undercut exists. Therefore, it is difficult to control the suspended length due to the undercut, and consequently, it is difficult to estimate the mechanical properties of the suspended SWNTs.

Another problem with wet etching is that it cannot be applied in general to low dimensional nanostructures other than CNTs, e.g. polymer nanofibres that can be damaged by the strong acid.

G. T. Kim et al. introduced a simple method to suspend CNTs and other nanowires without using wet etching [12].

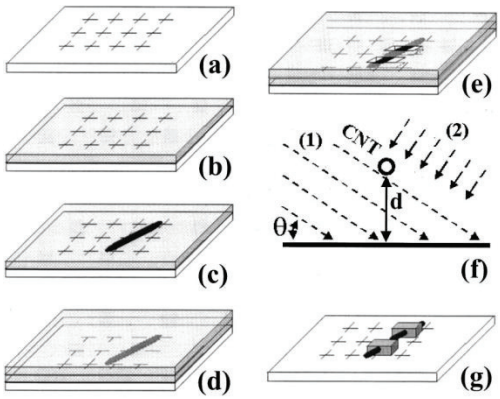

Figure 6. Schematic diagram of the process described by Kim et al. for preparing a suspended one dimensional nanostructure [12]. (Reprinted with permission from Appl. Phys. Lett.80, 1815 (2002). Copyright 2002 American Institute of Physics.)

Figure 6 shows the schematics of this process. The key idea is that the one-dimensional nanostructures are separated in advance from the substrate by placing a poly(methylmethacrylate) (PMMA) sacrificial layer between the deposited one-dimensional nanostructure and the substrate (see Fig. 6 (b) and (c)). An additional PMMA layer is spin-coated after deposition of SWNTs, resulting in the SWNTs being sandwiched by the two PMMA layers. The anchor structures are patterned by e-beam lithography and the developed PMMA area is replaced by metal. The evaporation should be done with a tilted angle so that the air gap under the suspended CNT at the developed area can be filled and, as a result, the CNT is anchored by the metal. It is possible to use this technique to produce a nano-gap electrode structure since the CNTs can be utilized as shadow masks [13] if evaporation occurs normal to the substrate. Using this method, it is possible to avoid the materials being exposed to strong acid so that the choice of low-dimensional nanomaterials for NEMS can be extended; any materials that are not damaged by organic solvents such as acetone or isopropanol can be used. However, since the CNTs have to be randomly dispersed on the sacrificial layer, usually only a single NEMS device can be fabricated at a time. The positional control of the nanostructure is one of the crucial issues for developing practical applications of NEMS for integration in future.

We have developed a method of producing suspended and aligned individual SWNTs using a combination of the ac dielectrophoresis technique and electron beam lithography. A PMMA sacrificial layer was used to make the suspended CNT structures without using an etching process. In this case, PMMA was selectively patterned so that it was used as a support between two Au electrodes to prevent the CNT from falling down onto the substrate. Ac dielectrophoresis is a widely used separation technique, especially in biology [14]. It has also been extensively used for depositing metallic CNTs [15]. This technique was applied in our work for positioning the CNTs between pre-patterned Au electrodes [16]. The PMMA sacrificial layer is only required in the region where the nanostructure should later be suspended. The PMMA was defined and fabricated using electron beam

lithography followed by development (Fig. 7(a) and (b)). The height of the PMMA was precisely reduced in a mild oxygen plasma to match the height of the Au electrodes pre-defined beside it (Fig 7.(c) and (d)). The CNT (or other one-dimensional nanostructure) is then aligned and deposited on the two Au electrodes by using ac dielectrophoresis (Fig 7. (e)). Besides controlling the position of the CNT, one can also control the number of aligned CNTs by controlling the density of the CNT suspension and by adjusting the applied ac field parameters such as amplitude, frequency, and application time etc. The suspended CNT structures are finally produced after evaporating upper electrodes to clamp the CNT in place, followed by a lift off process to remove the PMMA and critical point drying to avoid the collapse of the suspended structure (Fig 7. (f) and (g)). The detailed production procedure with optimized fabrication conditions was reported in ref [17].

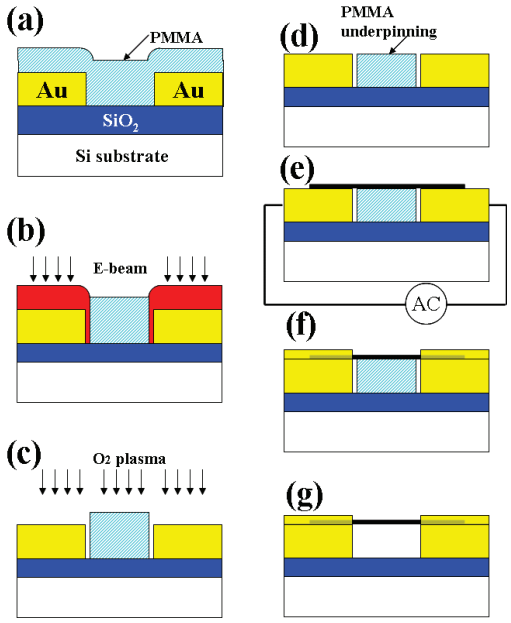

Figure 7.The sacrificial layer fabrication procedure for making suspended CNTs. Adapted from [17].

Three lithography steps are required for the fabrication; 1) patterning of Au electrodes, 2) fabrication of PMMA support, 3) defining upper electrode structure. This is one drawback of this process compared to the previous simpler methods. However, the method has several advantages. Firstly, it can be applied not only to CNTs but also to other low-dimensional nanostructures if they are resistive to organic solvents. Figure 8 shows scanning electron microscope (SEM) images of suspended structures made with different low-dimensional nanostructures [18]. Therefore, we can extend the field of electromechanical study to NEMS fabricated from various nanomaterials with this fabrication method.

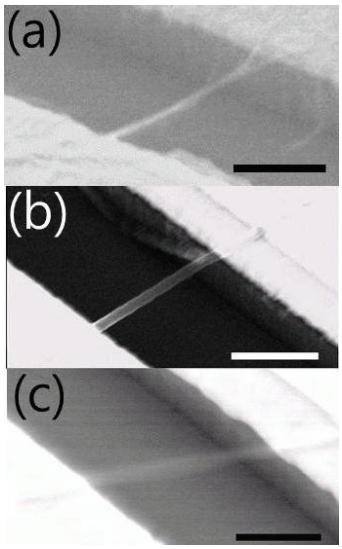

Figure 8. SEM images of suspended (a) CNT, (b) Polypyrrole (PPy) nanotube, and (c) Polyacetylene nanofiber. (Scale bar indicates 1 μm) [18] (Reprinted with permission from Nanotechnology 17, 992 (2006). Copyright 2006 IOP Publishing.)

Secondly, the dielectrophoresis technique makes it possible to position the nanostructures where we want to have them. Moreover, it is possible to make many electromechanical devices at once. The CNTs (or other nanostructures) can be aligned on each pair of electrodes simultaneously when an ac voltage is applied to one side of the electrode pairs in an array of devices [19]. Finally, this method makes it possible to pre-define the electrode structures under the suspended CNTs so that a variety of device geometries can be realised. Figure 9 shows carbon nanotube based NEMS that were fabricated by this method [20,21]. More than 2 electrode structures with different heights can be placed under the suspended CNTs. Each electrode can be used as a source of electrical signal to the CNT or as a probe for detecting the mechanical motion.

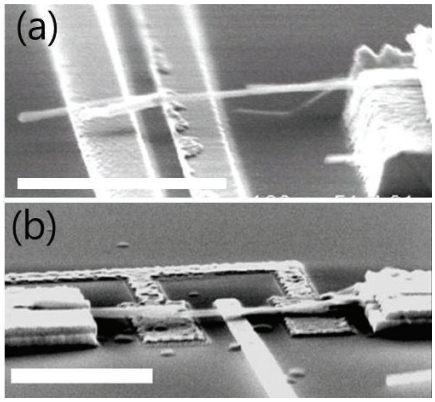

Figure 9. (a) 3 terminal carbon nano relay [20] (Reprinted with permission from Nanolett. 4, 2027 (2004). Copyright 2004 American Chemical Society.) (b) Doubly clamped suspended CNT based nano electromechanical switch [21] (Reprinted with permission from J. Kor. Phys. Soc. 55, 957 (2009). Copyright 2009.)

Besides these fabrication methods, CNT-based NEMS structures can be realized using nano manipulation techniques. A nano-manipulator can pick-up an individual CNT. The CNT can be attached to the end of the manipulator tip with conductive glue. The attached CNT can be freely suspended so that it is mechanically

movable as well as electrically connected through the manipulator. Several interesting NEMS were produced by using nano-manipulators such as CNT tweezers [22] and resonators [23,24]. This manipulation method has the advantage of an easy production process since the CNTs are freely suspended without considering the spatial constraint due to the substrate. However, it is not possible to make complicated structures, it is time-consuming and it is not a technique that can be easily up-scaled.

For all the fabrication techniques discussed so far, the CNTs have been prepared before the device fabrication. It is also possible to synthesize the CNTs after fabrication of other components. Steele et al have grown suspended SWNT using chemical vapor deposition (CVD) to realize resonator structures (Figure 10). In their work, the electrodes and the trench were pre-defined using lithography and wet etching. The suspended SWNT were grown by CVD as the last step of the device fabrication. In this case the suspended SWNTs are not influenced by etching or affected by any resist or other residues which might be attached to CNTs during the fabrication process. Therefore, very clean CNTs with few defects can be used for the devices so that more intrinsic electromechanical properties of the CNTs can be investigated.

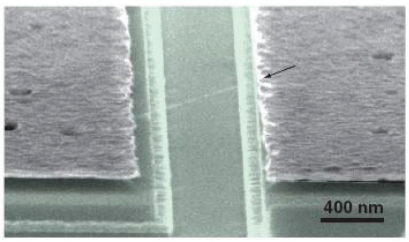

Figure 10. SEM image of Suspended SWNT based resonator fabricated by Steele et al [9]. (Reprinted with permission from Science 325, 1103 (2009). Copyright 2009 American Association for the Advancement of Science.) The CNT was grown by CVD at the last step of the device fabrication process.

Vertically aligned carbon nanofibre[i] (CNF)-based NEMS can be fabricated if the synthesis is carried out after defining the electrode structures [25]. Figure 11 shows a vertically aligned CNF NEMS switch. The two CNFs were vertically grown by using plasma-assisted CVD. Even though some additional processes were necessary to apply an insulating layer on one of the CNFs after growth, the electrode structures were defined before the CNF growth. Devices made with vertically aligned CNFs save space on the substrate so that they have an advantage for integrating nanodevices with electrical circuits.

[i] CNF have mechanical properties and dimensions that are similar to those of multiwalled CNT although they lack the perfect cylindrical geometry of true CNT. They are generally made by base-growth CVD from Ni particles and have sufficient mechanical stability to remain vertically-aligned as individual structures unlike true CNT.

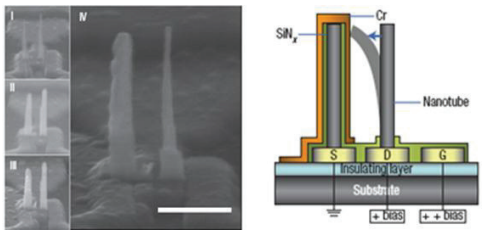

Figure 11. Nanoelectromechanical switch structure made of vertically aligned CNFs. [25] (Reprinted with permission from Nat. Nano. 3, 26 (2008). Copyright 2008 Nature Publishing Group.)

The processes for fabricating nanoelectronic and NEMS devices have been rapidly developed during the last decade. However, there is still need for improvement in the reliability and reproducibility of the mechanical and electrical properties of each fabricated NEMS. This is an important challenge if NEMS are to fulfill their promise as components of a post-Si technology.

3. Physical Properties of CNT Based NEMS

3.1 Mechanical measurements on suspended CNT

There are two methods which are widely used to measure the mechanical properties of CNTs and other low dimensional nanostructures; quasi-static measurements and dynamic measurements.

The force-distance measurement technique using atomic force microscope (AFM) tip manipulation is usually used for quasi-static measurements to determine the mechanical properties of suspended CNTs. Figure 12 shows the procedure of a force-distance measurement. The left part of Fig. 12 shows the shape of the cantilever during AFM tip manipulation in the AFM force measurement and the right part is the corresponding force-distance curve determined from the deflection of the cantilever. The x-axis represents the downward displacement of the AFM probe and the y-axis represents the voltage signal from the position sensitive photodiode (PSPD) which is directly related to the deflection of the cantilever. When the AFM cantilever approaches the sample and the tip touches the surface (Fig. 12 (a)), the cantilever is deflected. The voltage signal from the PSPD shows 0V when the tip contacts the surface of the sample. At the moment of contact, the cantilever bends down due to the adhesion force between sample and tip so that the PSPD signal decreases (Fig. 12(b)). The voltage signal of the photodiode will increase as the deflection of the cantilever increases (Fig. 12 (c)). In the retraction stage the cantilever feels the adhesion force between sample and tip (Fig. 12 (d)). When the tip is further retracted, it finally detaches from the surface and returns to its original status (Fig. 12 (e)). From the shape of the force-distance curve it is possible to estimate the mechanical character of the sample. For example, the force-distance curve will be a straight line if the surface of the sample is hard and it will be a curved line if the sample surface is soft. A large hysteresis between the forward and backward curve will be apparent if there is a strong adhesion force between tip and surface. The elastic modulus of a suspended sample can be calculated from the slope of the force-deflection curve which can be plotted after calibrating the spring constant of the AFM cantilever and extracting the net deflection of the suspended sample from the force-distance curve.

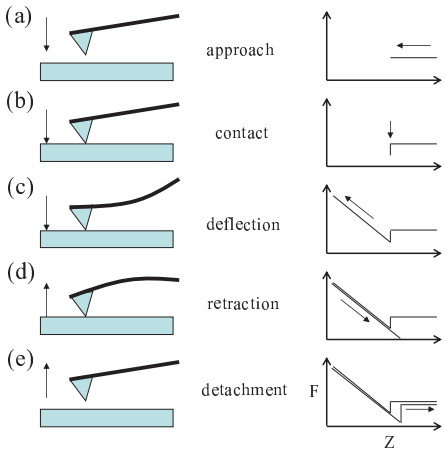

Figure 12.Cantilever movements during AFM force measurements and the corresponding force-distance curves.

The first application of this technique for determining the Young's modulus of an individual SWNT was reported by Walters et al. [26]. A SWNT was deposited on and clamped to the substrate and suspended by wet etching. The suspended SWNT was subsequently found by an AFM image scan. The AFM tip was moved to the centre of the suspended structure. The tip was then approached to the CNT and pushed down, using the force calibration mode (see Fig. 13). When the suspended CNT is pushed down with the AFM tip, both the cantilever of the AFM probe and the suspended CNT deflect together during the measurement. In order to determine the relationship between SWNT deflection and loading force, the cantilever deflection component needs to be extracted from the force-distance curve. The net deflection of the cantilever due to the applied force can be found by making a force calibration of the cantilever. This is done by making another force-distance measurement on the hard substrate with the same AFM probe. The pushing force versus the CNT deflection curve can be finally plotted after extracting the contribution of the cantilever deflection from the original force-distance curve.

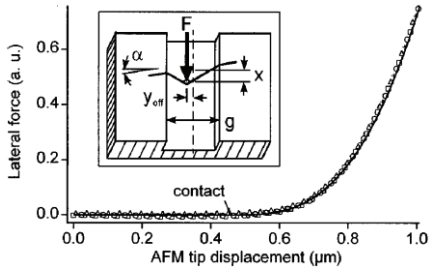

Figure 13.Force-distance measurement on a suspended CNT. Inset is a schematic figure of the device for measuring the mechanical properties of a CNT [26] (Reprinted with permission from Appl. Phys. Lett. 74, 3803 (1999). Copyright 1999 American Institute of Physics.)

Salvetat et al. [27] reported the results of measurements of the elastic moduli of individual suspended multiwall carbon nanotubes (MWNT) in the same year as Walters' report on SWNT [26]. The MWNTs were deposited on a polished ultrafiltration alumina membrane and the suspended structures were found by AFM imaging (see Fig. 14). The same AFM-deflection measurement, as described above, was carried out for various MWNTs. It was found that the modulus varied according to the defect concentration.

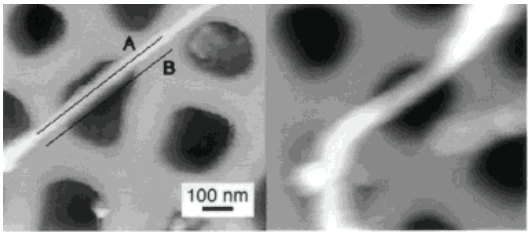

Figure 14. AFM images of MWNTs deposited on an alumina membrane [27] (Reprinted with permission from Adv. Mat. 11, 161 (1999). Copyright 1999 WILEY-VCH Verlag GmbH.)

The value of the elastic modulus for suspended one-dimensional nanostructures is extracted from the AFM deflection measurements by fitting the force-displacement curves to the expressions derived for appropriate mechanical models. A string model or a doubly-clamped beam model are usually used for extracting the mechanical properties of CNTs. The string model is typically used to estimate the mechanical properties of SWNTs and the beam model is often used for MWNTs, CNF or bundles of CNTs.

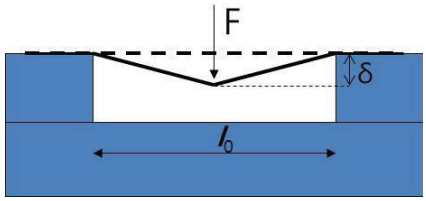

Figure15. Schematic figure of string model

If we assume that the suspended one dimensional structure is stretched when a loading force is applied, the material can be treated as an elastic string with extensional spring constant k and tension $T = k(l - l_0)$, where l is its stretched length and l_0 is its original length. A schematic illustration for the string model is shown in figure15. This figure is simplified by assuming that the loading force is applied to the middle part of the suspended string and that the suspended string is horizontal, without any slack. (The more general case that considers other factors is described in ref [26]). Then the stretched length l is given by:

$$l = \sqrt{l_0^2 + 4\delta^2}$$

where l_0 is the length of the trench and δ is the vertical displacement of the string when the loading force is applied. The tension is expressed as

$$T = k\left(\sqrt{l_0^2 + 4\delta^2} - l_0\right)$$

and from the equilibrium relation between the tension and the force, the relationship between the force and the deflection is expressed as

$$F = 2Tsin(\theta) = 2T\frac{2\delta}{l} = 8k\delta\left(\frac{\delta}{l}\right)^2 + O\left(\frac{\delta}{l}\right)^4$$

Finally we can see that the force scales as the cube of the vertical deflection

$$F \propto \delta^3$$

for small values of the displacement, δ. The elastic modulus, E, can then be estimated from the relationship:

$$F = 8EA(\delta/l)^3$$

where A is the cross section of the SWNT and we have used the relationship, $k = EA/\ell$.

The other widely used model for studying the mechanical properties of one dimensional nanostructures is the doubly-clamped beam model. This model is usually used for thicker nano structures such as MWNT, CNF or other nanowires where the displacement scales linearly with the applied force.

When a loading force is applied to a suspended beam in the vertical direction, the beam can be bent as

shown in Fig. 16 (a). There is one plane in the bent beam which has the same cross sectional length as the plane of the initial beam. The dashed line indicates the neutral line which means the cross section line of that plane. When the suspended beam bends, the upper part shrinks while the lower part expands with respect to the neutral line. The further away one is from the line, the more horizontal force is necessary for shrinking and expanding (Fig. 16 (b)). This difference between the two directions of horizontal force generates momentum. In the doubly-clamped beam system, the same amount of force will be applied by the clamping region as a reaction to the momentum of the beam. Therefore both components should be considered when estimating the relationship between displacement and force. As shown in figure 16 (c), the displacement y_1 due to the loading force F is expressed as [28]

$$y_1 = \frac{F}{48E} \cdot \frac{l^3}{I}$$

Where E is the elastic modulus, l is the length of the suspended beam, and I is the moment of inertia.

The relationship between displacement y_2 and the reactive force from the clamping region is

$$y_2 = \frac{M}{8E} \cdot \frac{l^2}{I} = \frac{F}{8E}\frac{l}{8} \cdot \frac{l^2}{I} = \frac{F}{64E} \cdot \frac{l^3}{I}$$

Therefore the resultant equation that relates force and displacement is expressed as

$$y = y_1 - y_2 = \frac{F}{E} \cdot \frac{l^3}{I}\left(\frac{1}{48} - \frac{1}{64}\right) = \frac{F}{192E} \cdot \frac{l^3}{I}$$

Using this equation, the elastic modulus of the suspended one-dimensional structure, typically MWNT or other nanowires, can be estimated from the force-displacement measurement results.

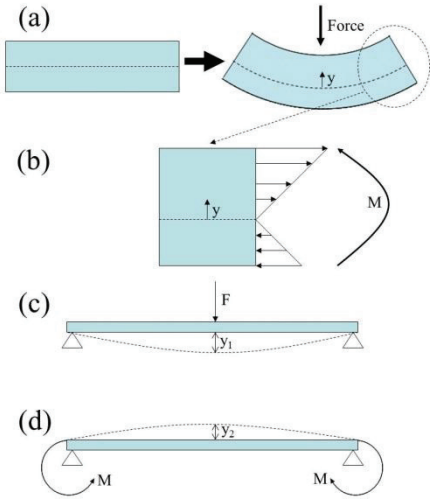

Figure 16.Schematics of beam model. (a) Before and after the force was loaded on the center of the suspended beam. (b) The expanding and shrinking factors due to the deformation. (c) Deflection (y_1) due to the loading force. (d) Deflection (y_2) due to the reactive momentum.

The mechanical properties of CNTs can be investigated also by dynamical measurements, e.g. observation of vibrational behaviour. The major difference between the dynamic measurements and the static ones is that a time-dependent term has to be added to the model [29]. A time-dependent external force is applied to the suspended structure and its torsional or flexural motions can be observed. The mechanical properties can be extracted from comparison of the experiments with the dynamical equation of motion.

The *in-situ* mechanical vibration of a carbon nanotube was first observed by using transmission electron microscopy (TEM) [30,31]. A suspended CNT which was singly-clamped to an electrical lead was prepared inside a TEM chamber. A counter-electrode was used to apply an alternating potential that induced the mechanical motion of the CNT.

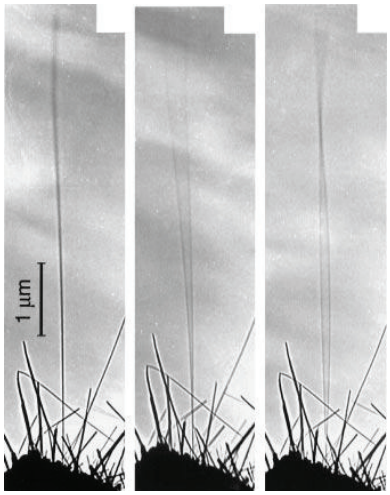

Figure 17.TEM images of CNT when it was under no potential, the fundamental mode, and the second harmonic mode of vibration respectively.[30] (Reprinted with permission from Science 283, 1513(1999). Copyright 1999 American Association for the Advancement of Science.)

Mechanical vibration modes of the CNT could be observed directly *in-situ*, as shown in figure 17. This method has the advantage that the mechanical vibration modes can be directly observed using the electron microscope. However, the electron beam, with high acceleration energy, can easily damage the nanostructures and it is possible that the physical properties of the CNT could be changed during the measurements.

The mechanical resonance modes of singly clamped CNTs can also be investigated by observing the field emission trajectory during their vibrations [32]. Purcell et. al prepared a suspended MWNT at the end of a metal tip inside a vacuum chamber for the field emission experiment. A schematic figure of the experimental set up is shown in figure 18. The MWNT can be vibrated by applying an ac signal to the side electrodes. A negative bias voltage was applied to the Ni tip to generate electron emission at the tip of the suspended MWNT. The mechanical resonance frequency of the MWNT was detected by observing a sudden size change of the field emission spot on the screen when the MWNT vibration is resonantly excited.

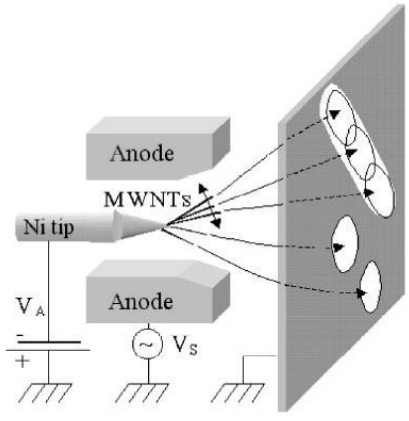

Figure 18.Schematic of measurement setup for measuring the resonance behavior of MWNT using field emission [32]. (Reprinted with permission from Phys. Rev. Lett. 89, 276103 (2002). Copyright 2002 American Institute of Physics.)

The vibrational modes of suspended CNTs can be electrically detected as well. The resonance frequencies of

doubly clamped suspended SWNT were detected in an electrical circuit by using the SWNT as a frequency mixer [33,34].

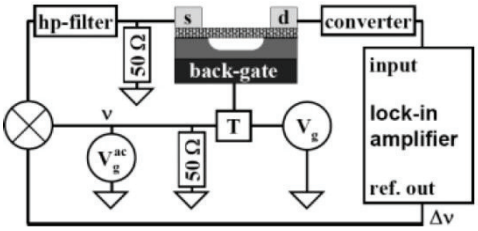

Figure 19.Schematic figure of the measurement setup for detecting mechanical resonance with an electrical method.[34] (Reprinted with permission from Nanolett. 6, 2904 (2006). Copyright 2006 American Chemical Society.)

Two ac signals that have frequencies $f - \Delta f$and $f + \Delta f$ were used for the measurement. The suspended SWNT was electrostatically actuated by one of the ac signals applied to the gate electrode. The gate capacitance is changed when the distance between the SWNT and the gate electrode changes due to the mechanical actuation. Since a semiconducting SWNT was used in this experiment, the transconductance of the SWNT changes when the SWNT vibrates in phase with the applied ac signal. Measuring the conductance change in the high frequency regime is a difficult task due to the low signal output and parasitic oscillations from the circuit. If another ac signal, with a slightly different frequency from that applied to the gate, is applied to the SWNT, mixed current signals with frequencies Δf, $2f + \Delta f$, and $2f - \Delta f$ will flow through the SWNT. The resonance mode of the SWNT can be detected easily in the low frequency regime when Δf is chosen to be low enough to detect with a lock-in amplifier.

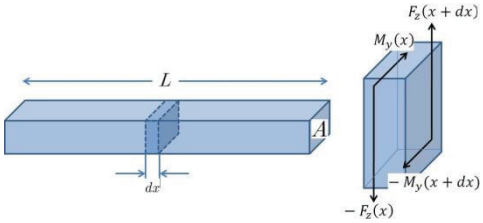

Figure 20. Model structure for the dynamic flexure measurement.

Once the mechanical resonance frequencies are measured, the elastic modulus of the CNT can be estimated by solving the equation of motion for dynamic flexural vibrations [29]. Figure 20 shows a simplified model structure to construct the relation between the displacement of a beam and the force applied to the beam. Note that the force applied to the beam is not static but alternates in the z-direction. No rotational motion is considered in the simple model. If we consider the displacement of a segment *dx* in a beam, *D(x,t)*, the equation of motion at *dx* is expressed as:

$$F_z(x+dx) - F_z(x) = d(ma) = dm \cdot \frac{d^2D}{dt^2}$$

where $dm = \rho A dx$, *a* is acceleration, and *D* is displacement.

Since the absence of rotational motion is assumed, the equation for the torque at *x* is expressed as

$$F_z(x+dx)dx = M_y(x) - M_y(x+dx)$$

The two equations can be simplified when we take the first order terms of the Taylor series, which are

$$\frac{\partial F_z}{\partial z} = \rho A \frac{\partial^2 U}{\partial t^2}$$

$$F_z(x) = \frac{\partial M_y}{\partial x}$$

where U is the time dependent transverse displacement.

Using the Euler-Bernoulli theory of beams [35], the torque term is given by

$$M_y = EI \frac{\partial^2 U}{\partial x^2}$$

where E is the elastic modulus of the beam and I is its moment of inertia.

When the torque term is applied to the two equations of motion, the resultant wave equation can be expressed as follows

$$\frac{\partial^4 U}{\partial x^4} = -\beta^4 U \qquad \beta^2 = \sqrt{\frac{\omega^2 \rho A}{EI}}$$

The general solution of $U(x)$, obtained by solving the above differential equation is expressed as

$$U(x) = a\,cos(\beta x) + b\,sin(kx) + c\,cosh(kx) + d\,sinh(kx)$$

The boundary conditions at x=0 and x=L (where L is the length of the suspended beam or string)

$U(0) = 0,\ \left.\frac{d^2U(x)}{dx^2}\right|_{x=0} = 0$ (at x=0)

$U(L) = 0,\ \left.\frac{d^2U(x)}{dx^2}\right|_{x=L} = 0$ (at x=L)

are applied to the solution.

The characteristic equation is finally expressed as

$$\sin \beta L = 0$$

and the solution of this equation is

$$\beta_r L = k\pi \quad k = 1, 2, \ldots$$

yielding the fundamental frequencies

$$\omega_k = (k\pi)^2 \sqrt{\frac{EI}{\rho A L^4}}$$

By measuring the resonance frequencies of the suspended CNT, we can investigate various dynamic phenomena as well as the Young's modulus.

3.2 Electromechanical measurement of CNT based NEMS

The same classification of measurement methods (quasi-static and dynamic), introduced for measuring

mechanical properties of CNT in the previous section, can be made for investigating the electromechanical properties of CNT.

Atomic Force Microscopy (AFM) is often used for quasi-static electromechanical measurements of CNTs. Tombler et. al first reported *in situ* conductance measurements while a partly suspended SWNT was pushed by an AFM tip [10]. It was observed that the conductance of the SWNT decreased each time the AFM tip pushed down the tube. It was discussed that the electrical properties of the suspended SWNT were sensitively changed by its structural deformation or tensile strain. More systematic measurements were later carried out simultaneously by the Dai and McEuen groups [36,37].

Minot et. al used the AFM tip simultaneously for applying strain to the suspended SWNT and for applying an electrostatic gate bias [36]. Figure 21 shows the schematics of their experiment. The AFM tip was used to accurately control the amount of applied strain. The electromechanical response of the SWNT was monitored by measuring the conductance through the gold electrodes. A gate bias voltage was applied through the metal-coated AFM tip while it was straining the SWNT. Their measurement results showed that the energy gap of the SWNT was modified by the strain. Depending on the tubes, the band gap can be increased or decreased under strain. A band gap could be opened in a metallic SWNT by applying strain.

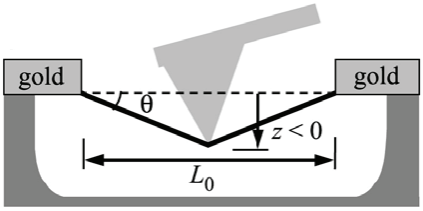

Figure 21.Experimental geometry for applying strain and gate voltage with an AFM tip, and measuring conductance with electrodes.[36] (Reprinted with permission from Phys. Rev. Lett. 90, 156401 (2003). Copyright 2003 American Institute of Physics.)

Cao et. al investigated the *in situ* electromechanical properties of suspended SWNT that were being stretched [37]. They fabricated a micromechanical structure (see Fig. 22) and grew an individual SWNT, using CVD, to bridge the gap between the end of the cantilever and the terrace structure. When an AFM tip pushes the micro cantilever in the downward direction, quasi-uniaxial strain is applied to the bridged suspended SWNT. Mo was deposited on the ends of the SWNT at both the cantilever and terrace sides so that the electrical characteristics of the suspended SWNT could be measured while it was stretched by the cantilever motion. Systematic electromechanical studies were carried out with various types of SWNTs.

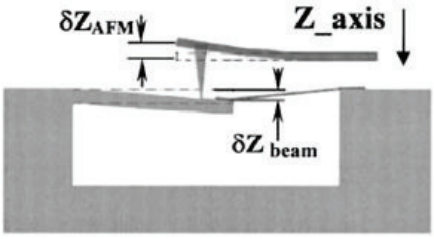

Figure 22. Scheme for *in situ* electromechanical measurement of suspended SWNT under stretch [37] (Reprinted with permission from Phys. Rev. Lett. 90, 157601 (2003). Copyright 2003 American Institute of Physics.)

Jungen et. al [38] reported similar studies on the electromechanical properties of a suspended SWNT attached to an electro-thermally operating MEMS actuator. It was observed that the current value of the suspended SWNT was sensitively changed by applying mechanical strain. The mechanical strain could be calibrated by comparing the actual mechanical displacement of the MEMS actuator. By using the MEMS actuators, this *in-situ* electromechanical measurement was performed by applying truly uniaxial strain to the SWNT, however, the focus was nore on the operation of the MEMS actuator than on the fundamental properties

of the SWNT.

A similar set-up to Cao et. al has been used to make *in situ* Raman measurements of SWNTs under quasi-uniaxial strain [39]. Raman spectroscopy is a powerful tool to probe the structural and electronic changes of CNT. A long micro-cantilever structure was used to avoid the screening of the laser beam in the Raman system by the AFM probe. Figure 23 shows an SEM image of the device and the measurement scheme for this experiment. The strain of the suspended SWNT was precisely controlled by the AFM tip at the middle of the cantilever. The Raman spectrum of the suspended SWNT was taken while strain was applied to the SWNT. The radial breathing mode (RBM) and G-band Raman peaks of suspended SWNTS were systematically measured from 0% to 1% strain.

These experimental studies clearly showed that the electronic properties of SWNT are very sensitively changed by mechanical strain. This implies that CNT can be used as highly sensitive electromechanical sensors or strain gauges by making use of their electromechanical properties.[40]

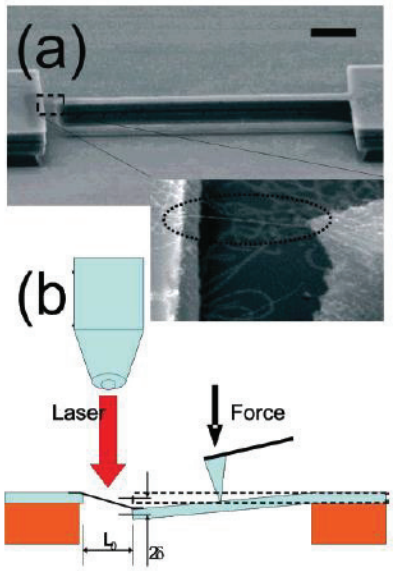

Figure 23. (a) SEM image of suspended SWNT attached to the micro cantilever and platform structure. (b) Schematics of the measurement set up. [38] (Reprinted with permission from Nanolett. 7, 2590 (2007). Copyright 2007 American Chemical Society.)

Studies of the electromechanical properties of CNT using dynamic measurements have been pursued to investigate quantum mechanical properties of electron transport through CNT-based nanoelectromechanical devices. For these studies, the experiments have focused on the coupling of tunneling transport and the mechanical motion of the CNT.[9] To observe quantum mechanical phenomena, the measurements should be done at low temperature. Realizing a CNT-based high frequency resonator with high Q factor is also important to detect sensitive electromechanical coupling phenomena. With improvements in fabrication and measurement techniques, it was possible to demonstrate CNT mechanical resonators with ultrahigh quality factors at low temperature under high vacuum conditions [41].

Based on these technical developments and the increasing knowledge of the dynamical properties of CNT, Steele et. al reported a strong coupling between electron tunneling and mechanical motion in a suspended SWNT structure [9]. The fabrication of the device structure was explained above, in the device fabrication section (see Fig. 10). A high quality factor, Q ~ 150000, made it possible to detect the shift of the resonance frequency caused by the addition of a single electron to the CNT. Figure 24 shows the evidence for the electro-mechanical coupling of the electron in the suspended CNT resonator. At low temperature (20 mK), a quantum dot structure was formed on some part of the suspended SWNT. When the gate voltage was increased in this CNT quantum dot device, periodic current peaks appeared due to Coulomb blockade (Fig. 24 a). The mechanical resonance frequency of the CNT was simultaneously measured while the gate voltage was increased

on the CNT. When a single electron was added to the suspended CNT, the total charge on the CNT increased and, as a result, the tension of the suspended CNT increased. Therefore the spring constant of the CNT increased, thus increasing the resonance frequency of the CNT (Fig. 24 b).

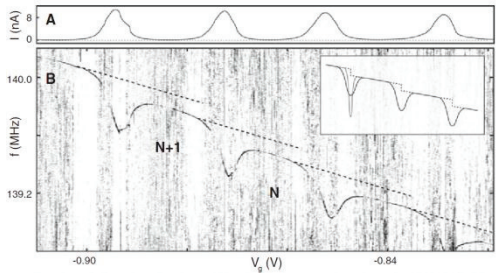

Figure 24. (a) I–V_g characteristics of suspended SWNT device which shows Coulomb blockade effect. (b) Resonance signal versus frequency and gate bias measured on the CNT resonator.[9] (Reprinted with permission from Science 325, 1103 (2009). Copyright 2009 American Association for the Advancement of Science.)

Besides this effect, the device showed damping and nonlinear behavior of the mechanical motion, which originated from energy transfer to the electron when it moves to the CNT. It was also observed that the direct current flow through the CNT could provide a force to change its mechanical motion.

This is the first experimental result that observes the electro-mechanical coupling of an electron in the quantum mechanical regime using CNT-based NEMS. As mentioned in the introduction, CNTs have both electrically and mechanically superior properties. For this reason, CNT based NEMS are promising systems that allow very sensitive measurements and even the investigation of quantum electro-mechanics [3,42].

4. Applications

As mentioned in the introduction, CNTs have a high Young's modulus and excellent stiffness combined with low mass. Because of these superior mechanical properties as well as versatile electrical properties, CNTs are considered to be promising candidates for electromechanical applications. In the following section, we will focus on a number of potential applications for CNT based NEMS in electronics, without aiming to give a comprehensive review.

4.1 RF components

Several groups have demonstrated the detection of mechanical vibration of CNTs using dynamic measurements, as introduced in section 3.1.[29-33] The reported resonance frequencies of CNTs vary from several MHz to a few hundred MHz. Another interesting and promising mechanical property of CNTs is that their mechanical resonance frequencies can be widely tuned by applying a tension to suspended CNTs.[33,43] This tunability of the mechanical resonance of CNTs in the RF regime opens up the possibility of CNT-based wide-range tunable RF components such as tunable filters, voltage controlled oscillators, nano transceivers, and so on.

Theoretical modeling first suggested RF applications of CNT by introducing a CNT relay structure [43-45]. The simulations showed that for a small, defect-free CNT, the mechanical resonance appears in the several GHz regime and the frequency can be tuned by more than factor of two by applying a DC bias voltage on the order of one volt.[43] The relay structure was experimentally realized [46] and RF transmission properties of this structure were also studied.[47] Eriksson et. al demonstrated the first direct electrical measurement of cantilever type CNF resonators using a broadband capacitive coupling technique. The observed resonance frequency tuning behavior was in good agreement with the predictions of the theoretical model.

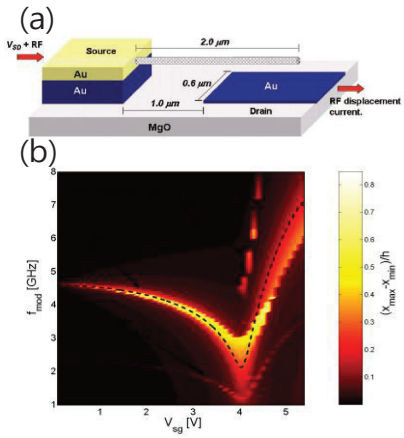

Figure 25. (a) Schematics of CNF relay structure [47] (Reprinted with permission from Nanolett. 8, 1224 (2008). Copyright 2008 American Chemical Society.) (b) Mechanical resonance frequency and tunability of CNT relay structure obtained by theoretical calculation.[43] (Reprinted with permission from Nanotechnology 15, 1497 (2004). Copyright 2004 IOP Publishing.)

Even though this work showed a promising possibility to apply CNT/CNF based NEMS for RF components, there are several technical challenges that need to be overcome before real applications are feasible. Firstly, the experimentally detected mechanical resonance frequency was much lower than the original theoretical prediction due to the fabrication practicalities, with the experimental relay having dimensions approximately one order of magnitude larger than the theoretical model. Secondly, the RF transmission signal from an individual nanostructure is too small for practical use and it would be necessary to work with arrays of structures [48]. The reason for the low output power is predominantly the 50Ω impedance mismatch, which is due to the high contact resistance between the CNT and metal electrode. These issues could be overcome by improving the device fabrication technique and controlling the growth so that arrays of identical structures could be grown.

A CNT radio is another interesting RF application that has been demonstrated [49, 50]. Jensen et. al reported that a single CNT resonator could operate as a radio by performing the role of all the essential Radio components, antenna, tuner and demodulator. (Fig 25) [49] To realize such a CNT-resonator-based radio, a cantilever type suspended CNT was used both as resonator and field emitter. When the modulation frequency matches the mechanical resonance frequency of the suspended CNT, the CNT will vibrate and, at the same time, demodulated current will pass from the end of the CNT to the anode via electron field emission. The sound signal can appear through a speaker after the current signal is amplified. Although this is a very nice demonstration, the practical applications are limited due mainly to the large electric field, on the order of kV, that needs to be applied to the CNT tip to induce electron field emission. The CNT radio demonstrated by Rutherglen and Burke [50] is more conventional in nature with a semiconducting CNT acting as the AM demodulator in the radio circuit, however, it does not make use of any mechanical resonance but relies on the highly nonlinear nature of the *I-V* behavior.

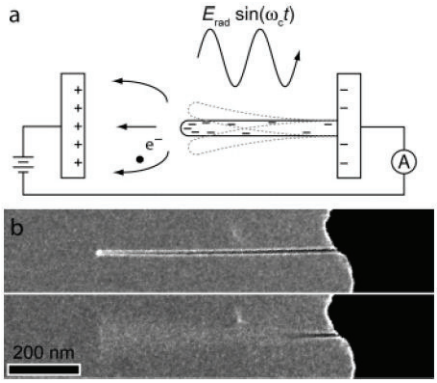

Figure 25. (a) Schematic of CNT Radio. (b) Transmission electron microscope of a cantilever type CNT resonator at off resonance (top) and on resonance (down). [49] (Reprinted with permission from Nanolett. 7, 3508 (2007). Copyright 2007 American Chemical Society.)

4.2 Vertically aligned CNT based varactor

In an electric circuit, reverse biased diodes are usually used for varactors. In order to adjust the capacitance of these devices, the thickness of the depletion layer of the diode is controlled by varying the applied reverse bias voltage. This is a useful component in electronic circuits but the devices do not perform very well in the RF regime. A novel device structure using electrically actuated vertically aligned CNTs was shown to operate as a varactor.[51] Fig. 26 shows the schematic layout and also an SEM picture of the fabricated CNT varactor. The geometry of the vertically aligned CNT array is defined by patterning a thin catalyst layer on the substrate (in this case Fe) and growing the CNT in the desired shape. As shown in Fig. 26, the synthesized CNT structures are singly clamped and have a parallel capacitor configuration. When a DC bias voltage is applied between the two CNT walls, the distance between the two walls can be changed by electrostatic actuation and, therefore, the capacitance of the device can be controlled. Since the conductance of CNT wall is comparable to that of metals but the density is much lower, it was possible to move the walls by applying just a few volts between them [51]. By comparing the experimental behavior with a model, it was possible to extract a value for the apparent Young's modulus of the capacitor walls assuming they could be treated as a low density metal. The extracted value was on the order of just a few MPa and thus orders of magnitude lower than for individual CNT. This is a consequence of the low density, "spaghetti-like" nature of the arrays allowing the individual nanotubes within the arrays to easily stretch and move with respect to their neighbours. The deflection at the top of the CNT walls scales as $1/\sqrt{(EI)}$ [52] so the very low effective Young's modulus was extremely favourable for achieving actuation with low applied voltages. The capacitance was determined from RF measurements and it was shown that even with the simple geometry shown in Fig. 26 it was possible to change reproducibly the capacitance by over 20%. Arun et al. fabricated a CNT varactor with a more complex geometry based on the work in [51], however, their CNT arrays were more dense and therefore much higher voltages were needed to achieve the same degree of actuation [53]. Clearly a compromise needs to be made between, on the one hand, having a sufficiently high CNT density to provide good definition of the geometrical structures[54] and, on the other hand, keeping the density sufficiently low to enable efficient low-power actuation.

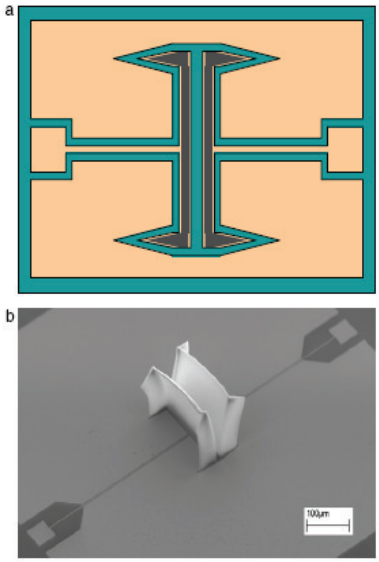

Figure 26. (a) Layout of the varactors substrate. (b) SEM picture of a directly grown varactor device. [51] (Reprinted with permission from Nanotechnology 20 385710 (2009). Copyright 2009 IOP Publishing.)

One of the biggest advantages of this device beside its RF compatibility is that the geometry of vertical CNT structure can be easily modified according to the specific electronic circuits by controlling the synthesis condition and catalyst patterns.

4.3 CNT based NEM memory

There are several candidates for the development of memory devices for the post-CMOS era such as FERAM, MRAM, PRAM, and ReRAM. The memory operations of those devices developed so far are achieved electronically. In the case of NEMS, however, the mechanical degrees of freedom can also contribute to the operation of the device so that versatile and novel properties may be expected from them. Only a few works have been reported that are concerned with the application of next generation memory devices using CNT based NEMS.

One of the first schemes suggested for a CNT based NEM memory was described by Rueckes et. al. [55] Fig. 27 (a) shows a schematic of their non-volatile random access memory based on CNT NEMS. The suspended CNTs act as bits that can be switched between an on- or off-state. The mechanical movement of the CNTs is controlled by electrostatic actuations. The reading and writing of the memory information is performed by measuring the current between the crossed CNTs at each bit position. It proved technologically challenging to produce large arrays of crossed, individual SWCNT. However, a company is now developing memories based on the same idea but using Buckypaper instead of individual CNT.[56]

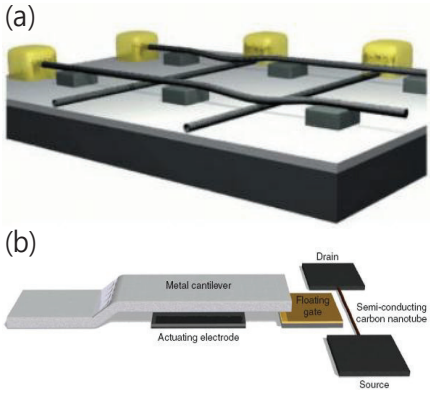

Figure 27 (a) Device architecture of CNT NEMS based non volatile random access memory [55] (Reprinted with permission from Science 289, 94 (2000). Copyright 2000 American Association for the Advancement of Science.) (b) Schematic diagram of the novel memory device consists of electromechanical switch and CNT transistor [57]

A different type of novel memory device has been demonstrated which is composed of an electromechanical system and a CNT field effect transistor.[57] The conventional flash memory cell consists of a CMOS transistor, a floating gate, and a control gate. The programming and erasing process of a flash memory are conducted by applying a high bias voltage through the control gate so that the charges are injected into or extracted out of the floating gate due to the tunneling effect. As shown in Fig. 28 (b), the programming and erase process of the memory device described in [57] is managed by the electromechanical switch, which can convey the electric potential through the floating gate by making direct mechanical contact. This device can be operated with very low power compared to flash memories since much less energy is necessary for inducing electromechanical switching than for inducing charge tunneling. Also the operational speed of this device is very fast because the speed of the device is mostly dependent on the speed of the mechanical switch. Much faster and lower power consuming memory would be expected if the present micro scale electromechanical switch could be replaced with a CNT NEM switch.

4.4 Tunable Photonic Crystal

The final example is a very recent demonstration of a tunable photonic crystal based on vertically aligned CNF [58]. Similar to the structures shown in Fig. 11, individual vertically-aligned CNF were grown on an electrode array to form a 2D photonic crystal with the ability to influence the transmission of visible light [59]. As in the varactor example, the CNF can be made to move by applying a voltage between the alternating polarity electrode strips. This changes the form factor of the photonic crystal and it is possible to monitor the changes in the optical properties via diffraction and ellipsometry experiments. Although the demonstrated change is rather small, this proof-of-principle experiment shows that a 2D photonic crystal, operating in the visible range, can be electrostatically actuated, opening up many possible applications within the field of optoelectronics.

5. Conclusion

Our understanding of NEMS has advanced considerably in recent years. The theoretical modeling is well established and has spurred experimental activity to explore ways of fabricating and characterizing electromechanical devices with nanoscale dimensions.

All of the examples of the application of CNT/CNF based NEMS reviewed in this paper showed superior device performance and present promising possibilities for future electronics. There are, however, some practical issues which need to be addressed before such NEMS devices can be competitive with or replace CMOS devices. The most important challenge is to obtain reliability and consistency in the fabrication of CNT/CNF based electromechanical devices. This issue is not only important for carbon-based NEMS research but is also relevant for the entire nano device research field. To produce reliable CNT/CNF based electromechanical devices with consistent operations, optimized device fabrication process and well controlled growth conditions should be established. The ability to control growth and to manipulate nanoscale structures is

developing rapidly and it can only be a matter of time before large scale fabrication and integration of NEMS becomes a reality.

Acknowledgements

We would like to thank all our students and collaborators over the years who have contributed to our CNT/CNF NEMS research, in particular our theoretical collaborators, Jari Kinaret and Andreas Isacsson from Chalmers University of Technology. The writing of this review was financially supported through BSR (2011-0021207, 2012R1A2A2A01045496), NMTD (2012M3A7B4049888), WCU (R31-2008-000-10057-0), and the framework of international cooperation programs supported by the National Research Foundation of Korea (NRF) funded by the Ministry of Education, Science and Technology

References

[1] J. W. Jewett, R. A. Serway, Principles of Physics (4th edit.) Brooks/Cole, a part of Cengage Learning, Inc. (2006)
[2] K. L. Ekinci, & M. L. Roukes, Nanoelectromechanical systems. Review of Scientific Instruments 76, 061101 (2005)
[3] K. C. Schwab, & M. L. Roukes, Putting mechanics into quantum mechanics. Physics Today 58, 36-42 (2005)
[4] Y. T. Yang, C. Callegari, X. L. Feng, K. L. Ekinci, and M. L. Roukes, Nanolett. 6, 583 (2006)
[5] A. K. Naik, M. S. Hanay, W. K. Hiebert, X. L. Feng and M. L. Roukes, Nature Nanotechnology, 4, 445 (2009)
[6] S. Iijima, "Helical microtubules of graphitic carbon". Nature 354 (6348): 56–58(1991).
[7] H. Maune and M. Bockrath "Elastomeric carbon nanotube circuits for local strain sensing" Appl. Phys. Lett. 89, 173131 (2006)
[8] J. Salvetat, G. A. D. Briggs, J. Bonard, R. Bacsa, A. J. Kulik, T. Stöckli, N. A. Burnham, and L. Forró "Elastic and Shear Moduli of Single-Walled Carbon Nanotube Ropes" Phys. Rev. Lett. 82, 944–947 (1999)
[9] G. A. Steele, A. K. Hüttel, B. Witkamp, M. Poot, H. B. Meerwaldt, L. P. Kouwenhoven, H. S. J. van der Zant, Science 325, 1103 (2009)
[10] T. Tombler, C. Zhou, L. Alexeyev, J. Kong, H. Dai, W. Liu, C. Jayanthi, M. Tang, S. Y. Wu. “Reversible Nanotube Electro-mechanical Characteristics Under Local Probe Manipulation,” Nature, 405, 769, 2000.
[11] J. Nygård and D. H. Cobden, "Quantum dots in suspended single-wall carbon nanotubes" Appl. Phys. Lett. 79, 4216 (2001)
[12] G. T. Kim, G. Gu, U. Waizmann, S. Roth, "Simple method to prepare individual suspended nanofibers", Appl. Phys. Lett. 80, 1815 (2002)
[13] J. Lefebvre, M. Radosavljević, and A. T. Johnson, "Fabrication of nanometer size gaps in a metallic wire" Appl. Phys. Lett. 76, 3828 (2000)
[14] H. A. Pohl “Dielectrophoresis”, Cambridge University Press, London, 1978
[15] R. Krupke, F. Hennrich, H. v. Löhneysen, M. M. Kappes "Separation of Metallic from Semiconducting Single-Walled Carbon Nanotubes" Science 301, 344 (2003)
[16] D. S. Lee, D. W. Kim, H. S. Kim, S. W. Lee, S. H. Jhang, Y. W. Park, E. E. B. Campbell, "Extraction of semiconducting CNTs by repeated dielectrophoretic filtering" Appl. Phys. A 80, 5 (2005)
[17] S. W. Lee, D. S. Lee, H. Y. Yu, E. E. B. Campbell and Y. W. Park, "Production of Suspended Individual Single-Wall Carbon Nanotubes Using the ac Electrophoresis Technique", Applied Physics A 78, 283-286 (2004)
[18] S. W. Lee, D. S. Lee, B. Kim, H. J. Lee, J. G. Park, S. J. Ahn, E. E. B. Campbell, Y. W. Park, “Fabrication and mechanical properties of suspended one dimensional polymer nanostructures: Polypyrrole nanotube and helical polyacetylene nanofiber.” Nanotechnology 17, 992 (2006)
[19] M. Ganzhorn , A. Vijayaraghavan , A. A. Green , S. Dehm, A. Voigt , M. Rapp , M. C. Hersam , and R. Krupke, "A Scalable, CMOS-Compatible Assembly of Ambipolar
Semiconducting Single-Walled Carbon Nanotube Devices" Adv. Mat. 23, 1734 (2011)
[20] S. W. Lee, D. S. Lee, R. E. Morjan, S. H. Jhang, M. Sveningsson, O. Nerushev, Y. W. Park, E. E. B.

Campbell, "A three-terminal carbon nanorelay", Nano Lett. 4, 2027 (2004)
[21] S. W. Lee, A. Eriksson, A. A. Sourab, E. E. B. Campbell, “Carbon-nanotube-based Nano Electromechanical Switches” J. Kor. Phys. Soc. 55, 957 (2009)
[22] P. Kim and C. M. Lieber, "Nanotube Nanotweezers", Science 286, 2148 (1999)
[23] K. Jensen, Ç. Girit, W. Mickelson, and A. Zettl. “Tunable nanoresonators constructed from telescoping nanotubes”. Phys. Rev. Lett. 97,215503 (2006)
[24] J. Cumings and A. Zettl. “Localization and nonlinear resistance in telescopically extended nanotubes”. Phys. Rev. Lett. 93, 086801 (2004)
[25] J. E. Jang, S. N. Cha, Y. J. Choi, D. J. Kang, T. P. Butler, D. G. Hasko, J. E. Jung, J. M. Kim & G. A. J. Amaratunga "Nanoscale memory cell based on a nanoelectromechanical switched capacitor" Nat. Nanotech. 3, 26 - 30 (2008)
[26] D. A. Walters, L. M. Ericson, M. J. Casavant, J. Liu, D. T. Colbert, K. A. Smith, and R. E. Smalley "Elastic strain of freely suspended single-wall carbon nanotube ropes " Appl. Phys. Lett. 74, 3803 (1999)
[27] J. P. Salvetat, A. J. Kulik, J. M. Bonard, G. A. D. Briggs, T. Stockli, K. Metenier, S. Bonnamy, F. Beguin, N. A. Burnham and L. Forro, “Elastic modulus of ordered and disordered multiwalled carbon nanotubes”, Advanced Materials 11, 161 (1999).
[28] S. P. Timoshenko, J. M. Gere, Mechanics of materials, D. Van Nostrand, NewYork(1972)
[29] A. N. Cleland “Foundation of Nanomechanics” Springer (2003)
[30] P. Poncharal1, Z. L. Wang, D. Ugarte and W. A. de Heer, “Electrostatic Deflections and Electromechanical Resonances of Carbon Nanotubes”Science, 283, p. 1513-1516(1999)
[31] R. Gao, Z. L. Wang, Z. Bai, W. A. de Heer, L. Dai, and M. Gao, “Nanomechanics of Individual Carbon Nanotubes from Pyrolytically Grown Arrays” Phys. Rev. Lett. 85, 622 (2000)
[32] S. T. Purcell, P. Vincent, C. Journet, and V. T. Binh, “Tuning of Nanotube Mechanical Resonances by Electric Field Pulling” Phys. Rev. Lett. 89, 276103 (2002)
[33] V. Sazonova, Y. Yaish, H. Ustunel, D. Roundy, T. A. Arias, and P. L. McEuen "A tunable carbon nanotube electromechanical oscillator," Nature 431, 284 (2004)
[34] B. Witkamp, M. Poot, and H. S. J. van der Zant, "Bending-Mode Vibration of a Suspended Nanotube Resonator" Nanolett 6, 2904 (2006)
[35] L. Meirovitch “Elements of Vibration Analysis”, McGraw-Hill (1986)
[36] E. D. Minot, Y.Yaish, V.Sazonova, J. Y. Park, M. Brink, and P. L. McEuen, “Tuning carbon nanotube bandgaps with strain” Phys. Rev. Lett. 90, 156401 (2003)
[37] J. Cao, Q. Wang, and H. Dai “Electromechanical Properties of Metallic, Quasimetallic, and Semiconducting Carbon Nanotubes under Stretching” Phys. Rev. Lett. 90, 157601 (2003)
[38]A. Jungen, C. Meder, M. Tonteling, C. Stampfer, R. Linderman, and C. Hierold, "A MEMS Actuator for Integrated Carbon Nanotube Strain Sensing," in Proceedings IEEE Sensors 2005, October 30-November 3, Irvine (CA), USA, pp. 93-96, 2005
[39] S. W. Lee, G. –H. Jeong, E. E. B. Campbell, “In-situ Raman measurement of suspended individual single-walled carbon nanotube under strain” Nanoletters 7, 2590 (2007)
[40] C. Stampfer, A. Jungen, R. Linderman, D. Obergfeld, S. Roth, C. Hierold, “Nano-electromechanical displacement sensing based on single-walled carbon nanotubes” Nanoletters 6, 1449 (2006)
[41] A. K. Huttel, G. A. Steele, B. Witkamp, M. Poot, L. P. Kouwenhoven and H. S. J. van der Zant, “Carbon Nanotubes as Ultrahigh Quality Factor Mechanical Resonators” Nanolett. 9, 2547 (2009)
[42] E. Buks, & M. L. Roukes, “Quantum physics: Casimir force changes sign” Nature 419, 119-120 (2002).
[43] L. M Jonsson, S. Axelsson, T. Nord, S. Viefers and J. M. Kinaret, “High frequency properties of a CNT-based nanorelay” Nanotechnology 15, 1497 (2004).
[44] L. M. Jonsson, T. Nord, and J. M. Kinaret "Effects of surface forces and phonon dissipation in a three-terminal nanorelay" J. Appl. Phys. 96, 629 (2004)
[45] J. M. Kinaret, T. Nord, and S. Viefers, "A carbon-nanotube-based nanorelay" Appl. Phys. Lett. 82, 1287 (2003)
[46] S. W. Lee, D. S. Lee, R. E. Morjan, S. H. Jhang, M. Sveningsson, O. Nerushev, Y. W. Park, E. E. B. Campbell, "A three-terminal carbon nanorelay", Nano Lett. 4, 2027 (2004)
[47] A. Eriksson, S. W. Lee, A. A. Sourab, A. Isacsson, R. Kaunisto, J. M. Kinaret, E. E. B. Campbell, "Direct Transmission Detection of Tunable Mechanical Resonance in an Individual Carbon Nanofibre Relay" Nanoletters 8, 1224 (2008)

[48] A. Isacsson, J.M. Kinaret, "Parametric resonances in electrostatically interacting carbon nanotube arrays" Phys. Rev. B 79, 165418 (2009)
[49] K. Jensen, J. Weldon, H. Garcia, and A. Zettl "Nanotube Radio" Nanolett. 7, 3508 (2007)
[50] C. Rutherglen, P. J. Burke "Carbon Nanotube Radio" Nano Letters, 7(11), 3296-3299 (2007)
[51] N. Olofsson, J. Ek-Weis, A. Eriksson, T. Idda and E. E. B. Campbell "Determination of the effective Young's modulus of vertically aligned carbon nanotube arrays: a simple nanotube-based varactor" Nanotechnology 20, 385710 (2009)
[52] L. D. Landau and E. M. Lifshitz, Theory of Elasticity, 2nd edn., Pergamon Press, Oxford. (1970)
[53] A. Arun, D. Acquaviva, M. Fernandez-Bolanosa, P. Salet, H. Le-Poche, T. Idda, R. Smajda, A. Magrezb, L. Forro, and A. M. Ionescu, in "MicroElectro-Mechanical Capacitors Based on Vertical Carbon Nanotube Arrays" (IEEE, Piscataway, 2009), pp. 335–338
[54] G. H. Jeong, N. Olofsson, L. K. L. Falk, E. E.B. Campbell, "Effect of catalyst pattern geometry on the growth of vertically aligned carbon nanotube arrays" Carbon 47, 696 (2009)
[55] T. Rueckes, K. Kim, E. Joselevich, G. Y. Tseng, C. L. Cheung and C. M. Lieber, Science 289, 94 (2000)
[56] See the following web page of Nantero company: http://www.nantero.com
[57] S. W. Lee, S. J. Park, E. E. B. Campbell, Y. W. Park, "A fast and low-power microelectromechanical system-based non-volatile memory device" Nat. Comm. Vol. 2, Article number: 220 (2011) (DOI:10.1038/ncomms1227)
[58] R. Rehammar, F. A. Ghavanini, R. Magnusson, J. M. Kinaret, P. Enoksson, H. Arwin, and E. E. B. Campbell "Electromechanically Tunable Carbon Nanofiber Photonic Crystal" Nanolett. DOI: 10.1021/nl3035527
[59] R. Rehammar, Y. Francescato, A.I. Fernandez-Dominguez, S. A. Maier, J. M. Kinaret, E. E. B. Campbell, “Diffraction from carbon nanofiber arrays” Optics Letters, 37 (1), 100 (2012)